1 2 AUG 1948

NATIONAL ADVISORY COMMITTEE
FOR AERONAUTICS

TECHNICAL NOTE

No. 1674

ESTIMATION OF EFFECTIVENESS OF FLAP-TYPE

CONTROLS ON SWEPTBACK WINGS

By John G. Lowry and Leslie E. Schneiter

Langley Aeronautical Laboratory
Langley Field, Va.

Washington
August 1948

NATIONAL ADVISORY COMMITTEE FOR AERONAUTICS

TECHNICAL NOTE NO. 1674

ESTIMATION OF EFFECTIVENESS OF FLAP-TYPE

CONTROLS ON SWEPTBACK WINGS

By John G. Lowry and Leslie E. Schneiter

SUMMARY

An analysis has been made of the low-speed lift, rolling, and
pitching characteristics of flap-type controls on a series of swept-
back wings, and methods are presented for estimating these characteristics.

The methods developed are essentially modifications of the existing
methods used in estimating the effectiveness of flap-type controls on
unswept wings. Satisfactory results may be obtained by each method for
flap-type controls on swept wings having from 0° to 60° sweep, aspect
ratios from 2.50 to 6.00, and taper ratios between 0.4 and 1.0. The
control parameters apply only in the range where the variations with
angle of attack and flap deflection are linear.

INTRODUCTION

In an attempt to extend the maximum speed of airplanes into the
transonic and supersonic speed range, an ever increasing number of
airplanes are being designed with swept wings. The use of these plan
forms has introduced the need for control-surface data on swept wings
similar to those already in existence for unswept wings (references 1
to 8), which allow for the prediction of control-surface characteristics
within small limits.

At the present time information on the behavior of controls in the
transonic speed range is too meager to permit the development of a rational
design procedure that applies at transonic speeds; hence, the design
of control surfaces for transonic airplanes must still be based primarily
on low-speed considerations.

A summary of the results of several low-speed wind-tunnel investi-
gations of control effectiveness on sweptback wings (data obtained in
the Langley 300 MPH 7- by 10-foot tunnel) and a discussion of the
development of two methods of estimating the effectiveness characteristics
of flap-type controls on sweptback wings are presented herein.

SYMBOLS

For the purposes of this paper, the chords and spans of the swept wings are measured parallel and perpendicular to the plane of symmetry, and the sweep angle is that of the wing leading edge (fig. 1). The control-surface deflections are measured in a plane perpendicular to the control hinge line. The term flap is used herein to designate any type of control surface, regardless of its application. The "unswept-" wing panel represents a wing that would be obtained if the swept wing were rotated about the midpoint of the root chord until the 50-percent-chord line is perpendicular to the plane of symmetry. The tip is cut off parallel to the plane of symmetry. The chords in this case are measured perpendicular to the 50-percent-chord line. All primed values refer to the "unswept" wing.

C_L wing lift coefficient (L/qS where L is lift of complete wing or twice lift of semispan wing)

c_l section lift coefficient

C_m wing pitching-moment coefficient ($M/qS\bar{c}$ where M is pitching moment of complete wing or twice pitching moment of semispan wing)

c_m section pitching-moment coefficient

C_l rolling-moment coefficient (L/qSb where L is rolling moment produced by deflection of one aileron on a complete wing)

S area of complete wing

b span of complete wing, measured on a line perpendicular to model plane of symmetry

b_f span of flap, measured on a line perpendicular to wing plane of symmetry

$\bar{c}$ wing mean aerodynamic chord $\left(\dfrac{2}{S}\displaystyle\int_0^{b/2} c^2 dy\right)$

c wing local chord, measured in planes parallel to model plane of symmetry

c_f chord of flap, measured in planes parallel to wing plane of symmetry

c_s wing root chord

λ wing taper ratio (Wing tip chord/Wing root chord)

y lateral distance from plane of symmetry

y_i lateral distance from plane of symmetry to inboard end of flap

y_o lateral distance from plane of symmetry to outboard end of flap

d distance from center of pressure of incremental lift load to moment axis, measured in planes parallel to wing plane of symmetry

A aspect ratio (b^2/S)

q free-stream dynamic pressure $\left(\frac{1}{2}\rho V^2\right)$

ρ mass density of air

V free-stream air velocity

α wing angle of attack, measured in model plane of symmetry

δ control-surface deflection, measured in a plane perpendicular to control-surface hinge line, positive when control-surface trailing edge is below wing chord plane

Λ wing sweep angle, that is, angle between wing leading edge and a perpendicular to wing plane of symmetry

α_δ flap effectiveness parameter, that is, effective change in wing angle of attack caused by unit angular change in control-surface deflection

$C_l/\Delta\alpha$ rolling-moment coefficient caused by a unit difference in wing angle of attack of various right and left parts of a complete wing

K_1 aspect-ratio correction factor for $C_l/\Delta\alpha$

K_2 taper-ratio correction factor for $C_l/\Delta\alpha$

K_3 aspect-ratio correction factor for $C_{l_\delta}/\alpha_\delta$

M Mach number (V/a)

a speed of sound

R Reynolds number $(\rho V \bar{c}/\mu)$

μ coefficient of viscosity of air

$$C_{L_\delta} = \left(\frac{\partial C_L}{\partial \delta}\right)_\alpha$$

$$C_{l_\delta} = \left(\frac{\partial C_l}{\partial \delta}\right)_\alpha$$

$$C_{m_\delta} = \left(\frac{\partial C_m}{\partial \delta}\right)_\alpha$$

The subscript α indicates the factor held constant. All slopes were measured or calculated in the range of $\alpha = 0^\circ$ and $\delta = 0^\circ$.

The rolling effectiveness parameter presented herein represents the aerodynamic effects on a complete wing produced by the deflection of the aileron on only one semispan of the complete wing. The lift and pitching effectiveness parameters represent the aerodynamic effects of deflection in the same direction of the flaps on both semispans of the complete wing.

EXPERIMENTAL DATA

In order to determine to what extent the design procedure for controls on unswept wings would have to be modified for swept wings, a semispan-wing model was tested essentially unswept ($\Lambda = 6.3^\circ$) and at sweep angles of 30°, 40°, and 51.3°. (See models 1 to 4, table I.) The aspect ratio of the wings varied from 6.23 for the 6.3° swept wing to 3.43 for the 51.3° swept wing. The wing was equipped with a variable-span plain-sealed flap having a chord 20 percent of the chord of the "unswept" wing. The tests were performed in the Langley 300 MPH 7- by 10-foot tunnel at a Mach number of about 0.12 and at Reynolds numbers of about 1.55×10^6 for the 6.3° swept wing and 2.2×10^6 for the 51.3° swept wing.

The variation of the rate of change of rolling-moment coefficient with deflection C_{l_δ} with span of aileron for the various angles of sweep, as obtained for models 1 to 4, is shown in figure 2. The aileron for these investigations extended inboard from the tip. The variation

of C_{l_δ} with sweep shown here also includes the effect of aspect ratio
which varied from 6.23 for the 6.3° swept wing to 3.43 for the 51.3°
swept wing. As the sweep is increased and as the aspect ratio decreases,
the values of C_{l_δ} decrease appreciably. In addition, the percent
decrease in the value of C_{l_δ} with increasing sweep is greater for short-
span tip ailerons than for ailerons of approximately 0.50 semispan or greater.

The lift effectiveness parameter C_{L_δ} obtained from these same
models showed about the same variation with sweep as did the rolling-
moment effectiveness parameter; that is, there was a decrease in C_{L_δ}
with increase in sweep and with decrease in aspect ratio. (See fig. 3.)
The pitching-moment effectiveness parameter C_{m_δ} showed about the same
variation with sweep as did the rolling-moment effectiveness parameter
except for the 6.3° swept wing (fig. 4). The linear variation of C_{m_δ}
with flap span on the 6.3° swept wing (fig. 4) and the drop-off of
effectiveness of the short-span tip flaps is the type of variation that
would be predicted from the theoretical treatment presented in reference 8.
The pitching moment produced by a given increment of flap span is propor-
tional to the product of the incremental lift produced by the flap and
the chordwise distance from the center of pressure of the incremental
load to the axis about which the moments are taken (the wing aerodynamic
center for these tests). The decreasing pitch effectiveness of a given
increment of span of flap for sweep angles greater than 30° indicates
that the incremental-lift-producing effectiveness of the flap decreases
faster than the moment arm of this incremental lift increases.

METHODS

The results of an analysis of the aforementioned wind-tunnel data
led to the development of two methods of estimating the lift and rolling
effectiveness parameters C_{L_δ} and C_{l_δ}, respectively, and one method
of estimating the pitching effectiveness parameter C_{m_δ}.

Method I

Rolling effectiveness parameter C_{l_δ}.— In order to make figure 2
of a more general nature, the data were reduced to a form similar to
that presented in reference 2 — that is, $C_l/\Delta\alpha$, the rolling-moment
coefficient caused by a unit difference in wing angle of attack of
various right and left parts of a complete wing. Simple sweep theory
indicates that only the component of the free-stream dynamic pressure q
in the direction perpendicular to the wing leading edge has a bearing
on the effectiveness of a flap; hence, the effective value of q at

constant free-stream velocity varies as $\cos^2\Lambda$. On this basis, the values of C_{l_δ} (fig. 2) at each spanwise station were divided by $\cos^2\Lambda$ and the value of the flap effectiveness parameter α_δ ($\Delta\alpha/\Delta\delta$ from reference 3) for the flap on the "unswept-"wing panel. No aspect-ratio or taper-ratio corrections were applied since the "unswept-"wing values of these factors for each of the swept wings are sufficiently near the aspect-ratio and taper-ratio values of the 6.3° swept wing to make corrections unnecessary. This reduction brought the curves into approximate agreement except for the short-span tip ailerons on the 40° and 51.3° swept wings. A curve of the average of the values computed from the curves of figure 2 and from the theoretical values of reference 2 for a comparable aspect ratio and taper ratio is presented in figure 5.

In order to use this chart for design purposes, the values must be corrected for aspect ratio, taper ratio, and flap chord. The rolling effectiveness parameter C_{l_δ} may be calculated from the formula

$$C_{l_\delta} = \left(\frac{C_l}{\Delta\alpha}\right)_u K_1 K_2 \alpha_\delta \cos^2\Lambda$$

The value of $\left(C_l/\Delta\alpha\right)_u$ can be obtained from the appropriate curve in figure 5 (the subscript u indicates the value of $C_l/\Delta\alpha$ for a wing of aspect ratio 6.00 and taper ratio 0.5); the aspect-ratio correction factor K_1 can be obtained from figure 6 and is the ratio of $C_l/\Delta\alpha$ for the aspect ratio of the "unswept" wing to the value of $C_l/\Delta\alpha$ for aspect ratio 6.00, both values being obtained from reference 2 for taper ratio 0.5; the taper-ratio correction factor K_2 can be obtained from figure 6 and is the ratio of the value of $C_l/\Delta\alpha$ for taper ratio of the "unswept" wing to the value of $C_l/\Delta\alpha$ for taper ratio 0.5, both values again being obtained from reference 2 for aspect-ratio 6.00; the flap effectiveness parameter α_δ is given in figure 7 and is based on the "unswept" flap chord ratio; and Λ is the sweep of the wing leading edge.

For sweep angles from 0° to 30°, values of $C_l/\Delta\alpha$ should be picked from the averaged curve in figure 5. Values for wings of higher sweeps may be obtained by interpolation between the averaged curve and the curve for the 51.3° swept wing. In order to calculate the rolling effectiveness of ailerons having chord ratios c_f'/c' which vary across the aileron span, the value of α_δ for the value of c_f'/c' at the inboard end of the aileron should be used.

The data of figure 2 and, hence, the curves of $C_l/\Delta\alpha$ of figure 5 apply to ailerons at spanwise locations other than those starting at the tip. The value of $C_l/\Delta\alpha$ for an element of aileron covering any spanwise part of the wing is the difference between $C_l/\Delta\alpha$ at the inboard end of the aileron and $C_l/\Delta\alpha$ at the outboard end of the aileron.

Lift effectiveness parameter C_{L_δ}.— The lift data presented in figure 3 were reduced to the parameter $C_{L_\delta}/\alpha_\delta$ by the same method used to reduce the roll data; that is, the value of C_{L_δ} at each spanwise station was divided by $\cos^2\Lambda$ and α_δ of the "unswept" control. This reduction brought all the data into general agreement except for the small span controls on the 51.3° swept wing which again showed a loss in lifting effectiveness. An averaged curve of $C_{L_\delta}/\alpha_\delta$ is presented in figure 8. The values of C_{L_δ} may be computed for wings of other sweep angles, aspect ratios, and flap spans by the formula

$$C_{L_\delta} = \left(\frac{C_{L_\delta}}{\alpha_\delta}\right)_u \alpha_\delta K_3 \cos^2\Lambda$$

The value of $\left(C_{L_\delta}/\alpha_\delta\right)_u$ is obtained from figure 8 (the subscript u indicates the value of $C_{L_\delta}/\alpha_\delta$ for a wing of aspect ratio 6.00 and taper ratio 0.5); the flap effectiveness parameter α_δ is obtained from figure 7; and the aspect–ratio correction factor K_3 is obtained from figure 9. The aspect–ratio correction factor K_3 is the ratio of the slope of the lift curve C_{L_α} of the "unswept" wing to the slope of the lift curve for a wing of aspect ratio 6.00. The data used in calculating this curve were obtained from complete models and isolated wings in the Langley 7– by 10–foot tunnel. No taper–ratio correction appears to be necessary, at least not for taper ratios of 0.4 to 1.0.

Lift data on unswept wings indicate that the lift effectiveness of flaps is different for flaps starting at the wing root and for those starting at the wing tip. Hence, it appears that this method must be limited to the prediction of the characteristics of flaps starting at the wing tip only.

Method II

Pitching effectiveness parameter C_{m_δ}.— Any attempts to correlate the pitching–moment data of figure 4 by methods similar to method I were unsuccessful. A method for calculating the pitching effectiveness

of partial span flaps is presented in reference 8. This method is based
on calculation of the theoretical spanwise load distribution by the
method of reference 1 and the chordwise location of the center of pressure
of each spanwise increment of this load. The pitching moment about the
wing aerodynamic center produced by this incremental load may then be
calculated at several spanwise stations and the resulting curve should
be integrated to determine the total pitching-moment effectiveness of
the flap. The method of reference 8 does not, however, take into con-
sideration any effects of sweep on the magnitude or distribution of the
spanwise loading.

On the basis of the results of the calculations of method I, it
appeared that unless sweep corrections were applied erroneous results
would be obtained if the method of reference 8 was used directly to
calculate the pitching effectiveness of flaps on highly swept wings.
The method presented in reference 8 was therefore revised to incorporate
such sweep corrections and is re-presented herein with the appropriate
sweep corrections applied.

The incremental lift caused by flap deflection at a constant angle
of attack was obtained by the influence-lines method of reference 1.
Inasmuch as the data of reference 1 apply rigorously only to wing
shapes shown in that report, a chord correction was necessary.
The spanwise loading factor $\dfrac{c_l(c/c_s)}{\alpha}$ at each spanwise station for
the wing in reference 1 most similar to the swept wing under considera-
tion with regard to taper ratio was multiplied by the ratio of the
chord of a wing having a straight leading and trailing edge, a square
tip, and a taper ratio the same as that of the wing in reference 1 to
the chord of the wing in reference 1. The two wings were compared in
such a manner that this ratio was 1.0 at the wing root.

The spanwise loading factors of reference 1 are presented for
several aspect ratios and taper ratios. The distribution of $\dfrac{c_l(c/c_s)}{\alpha}$
for the flap span under consideration, corrected for chord as previously
noted, was determined for each of the aspect ratios in reference 1 at
the taper ratio most nearly corresponding to the taper ratio of the
swept wing under consideration. The spanwise-load-distribution factors
presented in figure 2 of reference 1 are those produced by a flap
deflected on only one-half of a complete wing. In order to determine
the total spanwise loading on one-half of a complete wing caused by
deflection of a flap on both halves of the wing, the loading at a
negative (left) wing station must be added to the loading at the same
station on the positive (right) wing.

The values of the spanwise loading factor at each spanwise station
are then determined by extrapolation or interpolation of these data to
the aspect ratio of the "unswept" wing corresponding to the swept wing
under consideration.

The data of reference 1 give the value of incremental lift produced by flaps that create an effective change in angle of attack of 1 radian over the flapped part of the wing. It is assumed that the incremental lift produced by the flap is directly proportional to the effective angle of attack produced by the flap. Thus, in order to convert such data to the incremental lift produced by a different flap deflection, it is necessary to determine the incremental angle of attack produced by that flap deflection. As has been previously mentioned, the incremental angle of attack produced by flap deflection is indicated by the flap effectiveness parameter α_δ as shown in figure 7 for various percent-chord flaps. The incremental section lift coefficient Δc_l at each spanwise station produced by unit flap deflection may now be calculated by the following formula:

$$\Delta c_l = \frac{c_l(c/c_s)}{\alpha} \frac{\alpha_\delta}{57.3} \frac{c_s}{c} \cos^2\Lambda \tag{1}$$

where $\dfrac{c_l(c/c_s)}{\alpha}$ is the spanwise loading factor previously calculated from reference 1, α_δ is the flap effectiveness parameter (taken from fig. 7) of the flap having the chord ratio c_f'/c', c_s/c is the chord ratio of the wing in question, and Λ is the sweep angle of the wing leading edge.

The pitching-moment effectiveness parameter C_{m_δ} may be calculated by multiplying the incremental lift load at each spanwise station as computed by formula (1) by the corresponding moment arm — that is, the distance between the local center of pressure of the incremental lift load and the moment axis. Mechanical integration of the spanwise distributions of pitching moments thus obtained yields the total pitching effectiveness of the flap C_{m_δ}. The chordwise variation of the local center of pressure of the incremental lift load across the span of the wing was determined by a method, the reasoning behind which is discussed in detail in reference 8. Briefly, the method involves placing the line of centers of pressure of the incremental lift loads over the flapped part of the wing along the percent chord line (in the stream direction) indicated by the center-of-pressure data shown in figure 10. (The data in this figure were determined from the data of references 8 to 11.) The line of centers of pressure of the incremental lift loads over the unflapped part of the wing are laid out on a faired line which intersects the line of centers of pressure over the flapped part of the wing at the inboard end of the flap and become tangent to the wing quarter-chord line at a point approximately 30 percent of the wing semispan inboard of the inboard end of the flap, as shown in figure 11.

Lift effectiveness parameter C_{L_δ}.— The lift effectiveness parameter C_{L_δ} may be calculated as an incidental to the calculation of C_{m_δ} by mechanically integrating the area under the curve of Δc_l (determined by formula (1)) against spanwise location.

Rolling effectiveness parameter C_{l_δ}.— The rolling effectiveness parameter C_{l_δ} may also be computed. The same spanwise lift distribution used to determine C_{L_δ} may be mechanically integrated to determine the moment of the load about the wing center line. The rolling-moment coefficients so computed are somewhat in error since they include the carry—over effects of a flap deflected in the same direction on the remaining half of the complete wing. The rolling—moment coefficients so computed may be readily corrected for the carry—over effects by the method of figure 13 of reference 12. For illustrative purposes, a sketch of the incremental section lift and pitching—moment coefficients produced by a partial—span flap on a swept wing is shown in figure 11.

ACCURACY OF METHOD

In order to determine the reliability of the two methods of predicting the various control parameters on wings having various geometric characteristics, values of C_{L_δ} and C_{l_δ} were estimated by method I and values of C_{L_δ}, C_{l_δ}, and C_{m_δ} were estimated by method II for the wings shown in table I. These estimated values are compared with the experimentally determined values.

Comparisons of estimated C_{L_δ} with experimental C_{L_δ} and estimated C_{l_δ} with experimental C_{l_δ} are presented in figures 12 and 13, respectively, for method I and in figures 14 and 15, respectively, for method II. It appears from the scatter of points around the line of agreement that both methods give equally good agreement in calculating C_{L_δ}. For calculating C_{l_δ}, method I appears to give somewhat better agreement with the experimental results than does method II. In general, method II underestimates the rolling effectiveness. The spanwise—load—distribution factors presented in reference 1 are for wings with round tips, whereas all the experimental data used in the comparison are for wings having essentially square tips. The difference between the load on a wing with a round tip and the load on a wing with a square tip would be small in regard to lift or pitching moment. However, the load difference between the two wing shapes would be located near the wing tip and would consequently be expected to have some effect upon the rolling moments.

With the exception of the estimated values for models 2 and 15 (table I), the agreement of estimated C_{m_δ} with the experimental results was excellent, as is shown in figure 16.

It was noted in the correlation for method I that the lift and rolling effectiveness data for model 2 failed to correlate with the comparable data for models 1, 3, and 4, the results for model 2 being, in general, too high. The comparisons of calculated with experimental lift and rolling effectiveness shown in figures 14 and 15 for method II seem to substantiate the belief that the data for model 2 are in error. Since the lift, rolling, and pitching effectiveness of a given flap are so closely interrelated, it may also be assumed that the pitching effectiveness data of model 2 are also somewhat in error and hence would fail to correlate with the data of other models.

In general, it may be stated that both methods of calculating the control effectiveness parameters gave satisfactory results for sweptback wings having sweep angles from 0° to 60°, aspect ratios from 2.50 to 6.00, taper ratios from 0.4 to 1.0 and having conventional low drag or circular-arc airfoils. Both of these methods are, of course, limited to the range wherein lift has a linear variation with both wing angle of attack and flap deflection. As was previously mentioned, lift data on unswept wings indicate that the lift effectiveness of flaps is different for controls starting at the wing root than for controls starting at the wing tip. Hence, in addition to the aforementioned restrictions placed on both methods, method I must be limited to the prediction of the lift characteristics of flaps starting at the wing tip only.

It was found in estimating the control parameters for the various wings that C_{L_δ} and C_{l_δ} could be estimated in about 1/2 to 1 hour by method I and C_{m_δ} $\left(\text{and incidentally } C_{L_\delta} \text{ and } C_{l_\delta}\right)$ in about 3 to 4 hours by method II.

CONCLUDING REMARKS

An analysis has been made of the low-speed lift, rolling, and pitching characteristics of flap-type controls on a series of sweptback wings, and methods are presented for estimating these characteristics.

The methods of calculating the control effectiveness parameters give satisfactory results for sweptback wings having sweep angles from 0° to 60°, aspect ratios from 2.50 to 6.00, and taper ratios from 0.4

to 1.0. These methods are limited to the range wherein lift has a
linear variation with both wing angle of attack and flap deflection.

Langley Memorial Aeronautical Laboratory
    National Advisory Committee for Aeronautics
        Langley Field, Va., May 3, 1948

REFERENCES

1. Pearson, Henry A., and Jones, Robert T.: Theoretical Stability and Control Characteristics of Wings with Various Amounts of Taper and Twist. NACA Rep. No. 635, 1938.

2. Weick, Fred E., and Jones, Robert T.: Résumé and Analysis of N.A.C.A. Lateral Control Research. NACA Rep. No. 605, 1937.

3. Langley Research Department: Summary of Lateral-Control Research. (Compiled by Thomas A. Toll.) NACA TN No. 1245, 1947.

4. Ames, Milton B., Jr., and Sears, Richard I.: Determination of Control-Surface Characteristics from NACA Plain-Flap and Tab Data. NACA Rep. No. 721, 1941.

5. Crane, Robert M.: Computation of Hinge-Moment Characteristics of Horizontal Tails from Section Data. NACA CB No. 5B05, 1945.

6. Swanson, Robert S., and Crandall, Stewart M.: Lifting-Surface-Theory Aspect-Ratio Corrections to the Lift and Hinge-Moment Parameters for Full-Span Elevators on Horizontal Tail Surfaces. NACA TN No. 1175, 1947.

7. Fischel, Jack, and Ivey, Margaret F.: Collection of Test Data for Lateral Control with Full-Span Flaps. NACA TN No. 1404, 1947.

8. Pitkin, Marvin, and Maggin, Bernard: Analysis of Factors Affecting Net Lift Increments Attainable with Trailing-Edge Split Flaps on Tailless Airplanes. NACA ARR No. L4I18, 1944.

9. Street, William G., and Ames, Milton B., Jr.: Pressure-Distribution Investigation of an N.A.C.A. 0009 Airfoil with a 50-Percent-Chord Plain Flap and Three Tabs. NACA TN No. 734, 1939.

10. Ames, Milton B., Jr., and Sears, Richard I.: Pressure-Distribution Investigation of an N.A.C.A. 0009 Airfoil with a 30-Percent-Chord Plain Flap and Three Tabs. NACA TN No. 759, 1940.

11. Ames, Milton B., Jr., and Sears, Richard I.: Pressure-Distribution Investigation of an N.A.C.A. 0009 Airfoil with an 80-Percent-Chord Plain Flap and Three Tabs. NACA TN No. 761, 1940.

12. Swanson, Robert S., and Toll, Thomas A.: Jet-Boundary Corrections for Reflection-Plane Models in Rectangular Wind Tunnels. NACA ARR No. 3E22, 1943.

TABLE I.— SUMMARY OF GEOMETRIC CHARACTERISTICS OF MODELS USED IN ANALYSIS

[Data obtained from wind-tunnel investigations at the Langley Laboratory[a]]

	Model	Symbol notation for figures 12 to 16	Λ (deg)	Type of test	Airfoil reference line	A	λ	$c_f{}^1/c^1$	Location of control		Air-flow characteristics	
									$\frac{y_i}{b/2}$	$\frac{y_o}{b/2}$	M	R
	1		6.3	Semispan	"Unswept" 0.50c	6.23	0.49	0.20	0.71 .42 .05	0.99 .99 .99	0.12	1.55×10^6
	2		30	Semispan	"Unswept" 0.50c	5.26	.47	.184	.90 .67 .39 .05	.99 .99 .99 .99	.12	1.6
	3		40	Semispan	"Unswept" 0.50c	4.53	.46	.177	.87 .63 .35 .06	.99 .99 .99 .99	.12	1.8
	4		51.3	Semispan	"Unswept" 0.50c	3.43	.44	.167	.82 .59 .30 .06 .30 .06	.99 .99 .99 .99 .817 .585	.12	2.2
	5		35	Semispan	--------	6.0	.625	.272	.614	1.00	---	----------
	6		45.1	Complete model	$\frac{c}{4}$	2.50	.425	.20	.50	1.00	.12	2.05
	7		30	Complete wing	Wing L.E.	4.36	1.00	.20	.50	1.00	.17	1.15
	8		45	Complete wing	Wing L.E.	3.56	1.00	.20	.50	1.00	.17	1.40
	9		60	Complete wing	Wing L.E.	2.52	1.00	.20	.50	1.00	.17	1.98
	10		45	Complete wing	Wing L.E.	2.61	1.00	.20	.50	1.00	.17	1.4
	11		42.8	Complete model	$\frac{c}{4}$	4.00	.50	.20	.50	1.00	.16	2.15
	12		38.7	Complete model	$\frac{c}{4}$	4.51	.54	.14	.515	1.00	.16	1.8
	13		39	Complete model	--------	4.05	.54	.124	.515	1.00	.16	2.05
	14		38	Complete model	$\frac{c}{4}$	3.01	.60	Tip 0.28c Root 0.22c	.47	.96	.4	2.8
	15		42	Semispan	$\frac{c}{4}$	4.01	.62	.20	.51	1.00	.11	2.30
	16		42.8	Effectiveness of horizontal tail on complete model	--------	3.87	.49	.20	.04	1.00	.16	2.15

[a]Information for model 5 obtained from German investigation.
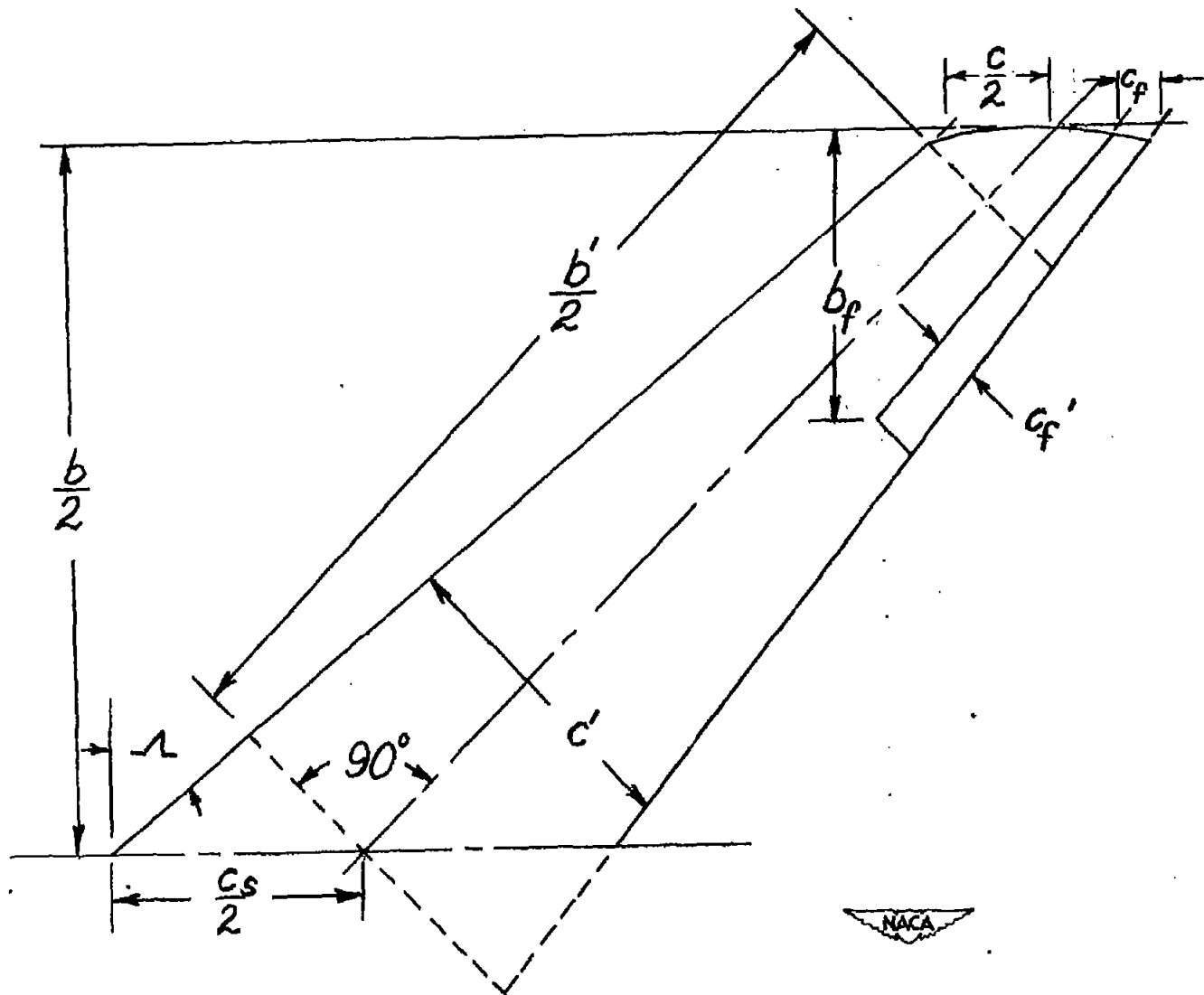
Figure 1.- Chords, spans, and sweep angle of swept and "unswept" wing.
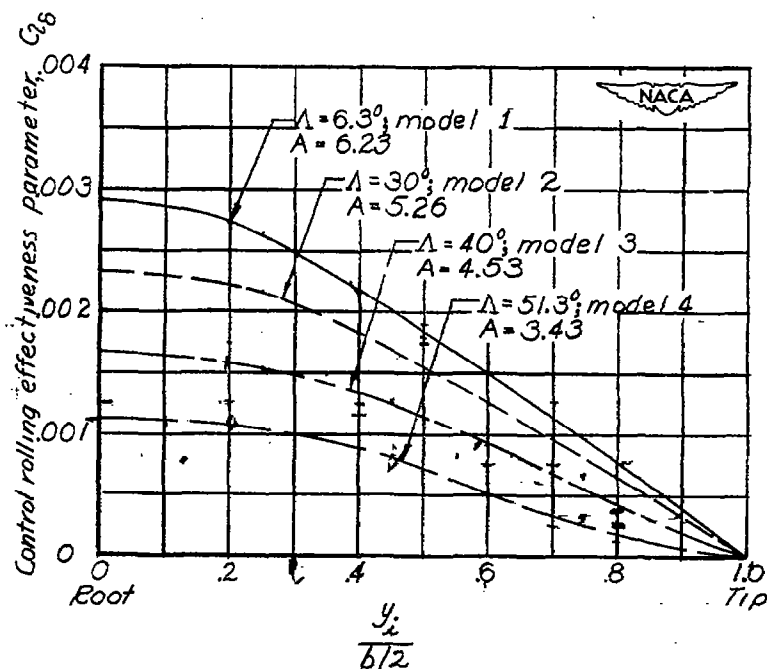
Figure 2.- Effect of sweep, aspect ratio, and span of control
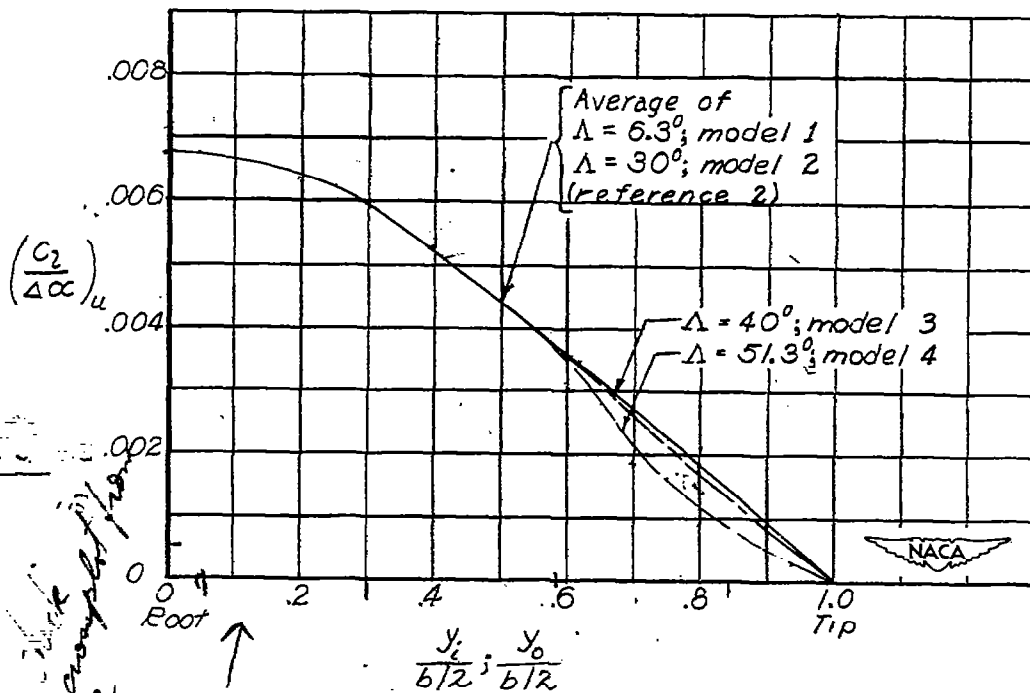on rolling effectiveness parameter. $\frac{y_0}{b/2}$ = 0.99.
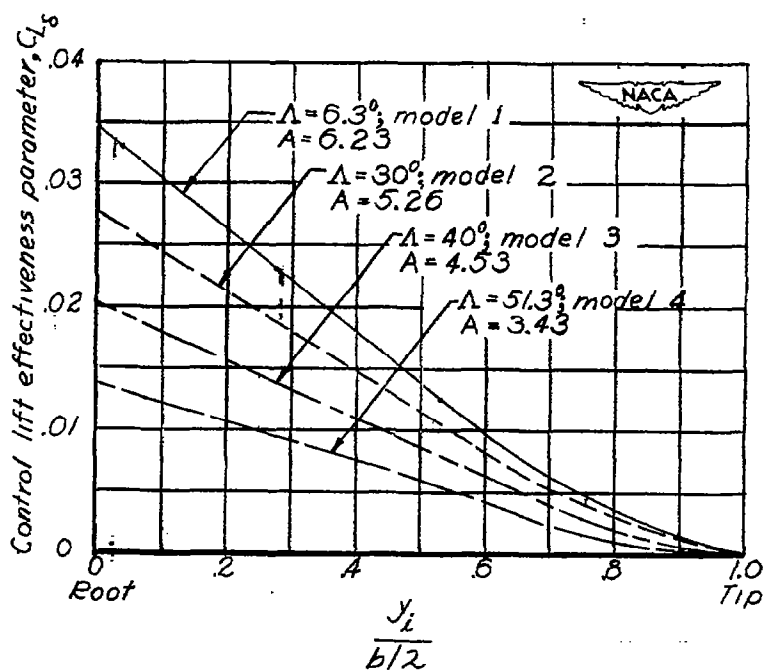
Figure 3.- Effect of sweep, aspect ratio, and span of control
on lift effectiveness parameter. $\frac{y_0}{b/2}$ = 0.99.

F-105 C_{l_δ} TN 1674 J. Lowry.

$$C_{l_\delta} = \left(\frac{C_2}{\Delta\alpha}\right)_u K_1 K_2 \alpha_\delta \cos^2 \Lambda$$

$(C_2/\Delta\alpha) = .0023$

$A' = 4.9$ $c_f'/c' = .296$ $\Lambda \approx 47.9°$

$\lambda' = .52$ $\cos 47.9° = .670$

$\cos^2 47.9° = .449$

$K_1 = .92$ $K_2 = 1.01$

$\alpha_\delta = .575$

$C_{l_\delta} = .0023 \times .92 \times .575 \times .449$

$= .00055$
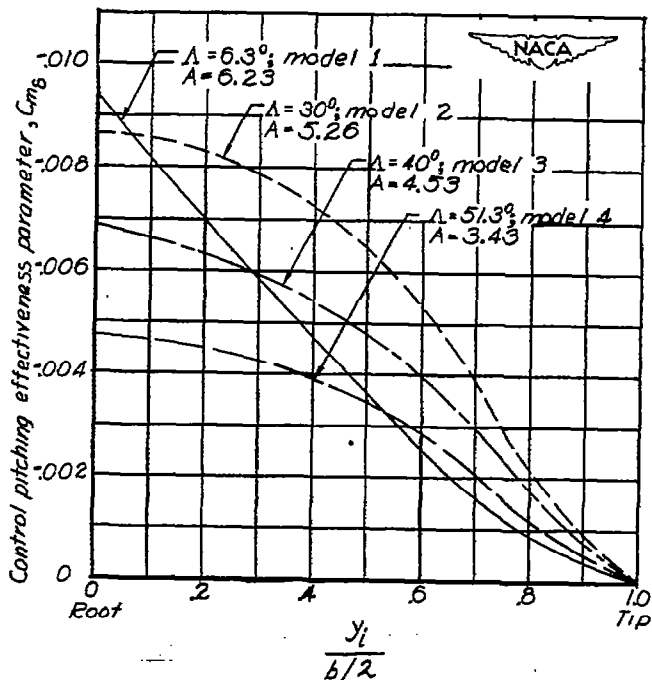
Figure 4.-   Effect of sweep, aspect ratio, and span of control

on pitching effectiveness parameter. $\frac{y_o}{b/2}$ = 0.99.

Figure 5.-   Variation of theoretical and experimental values

of $C_l / \Delta \alpha$ with flap span. $\bar{C}_{l_\delta} = \left(\frac{C_l}{\Delta \alpha}\right)_u K_1 K_2 \alpha_\delta' \cos^2 \Lambda.$
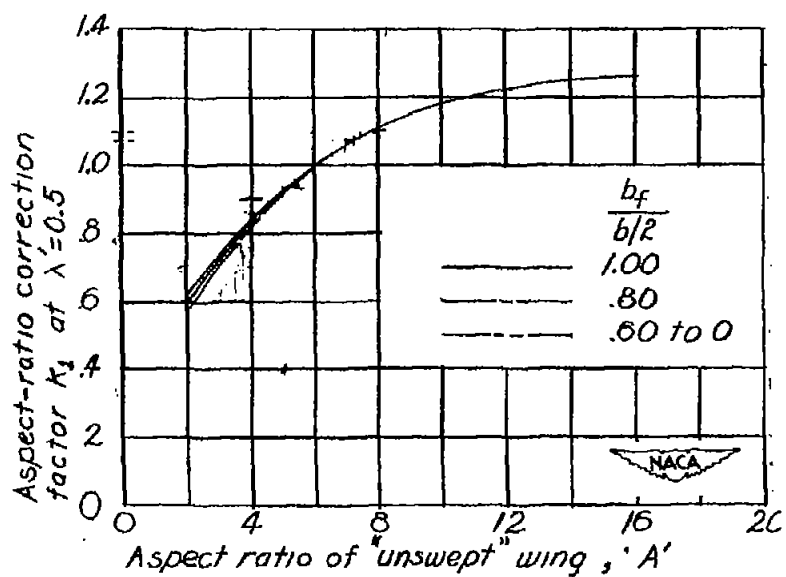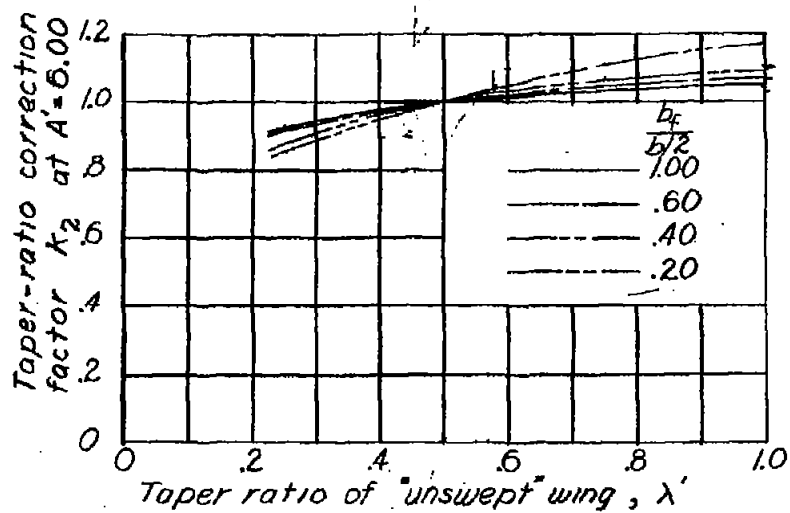
Figure 6.- Aspect-ratio and taper-ratio correction factors for calculating C_{l_δ}. (Curves calculated from data in reference 2.)
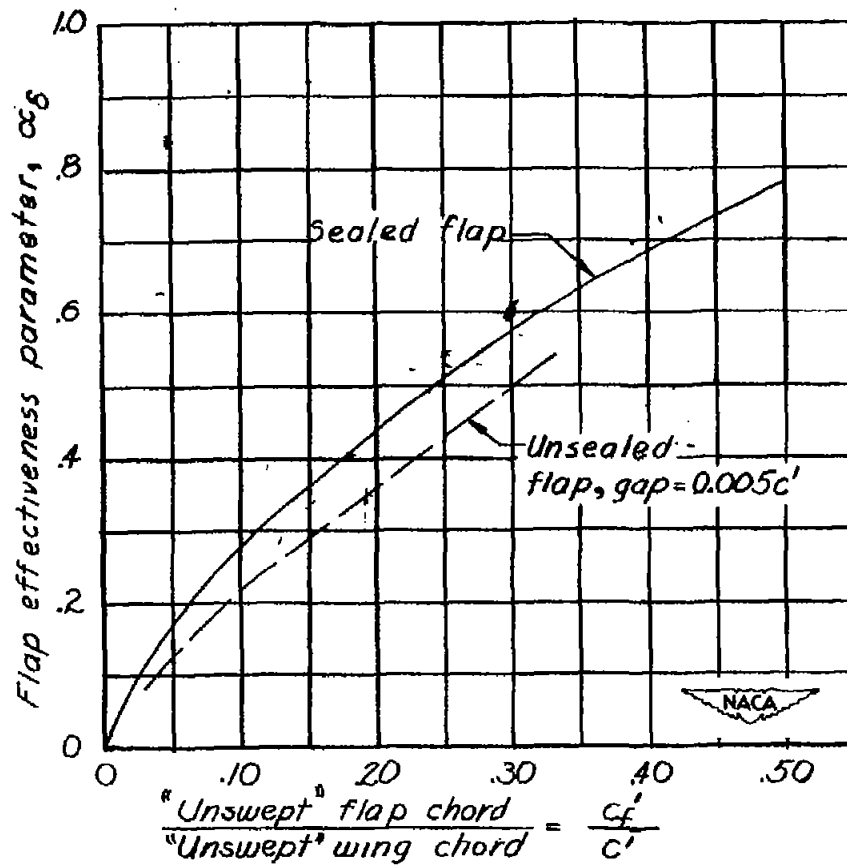
Figure 7.- Variation of flap effectiveness parameter with flap chord. (Data from reference 3.)
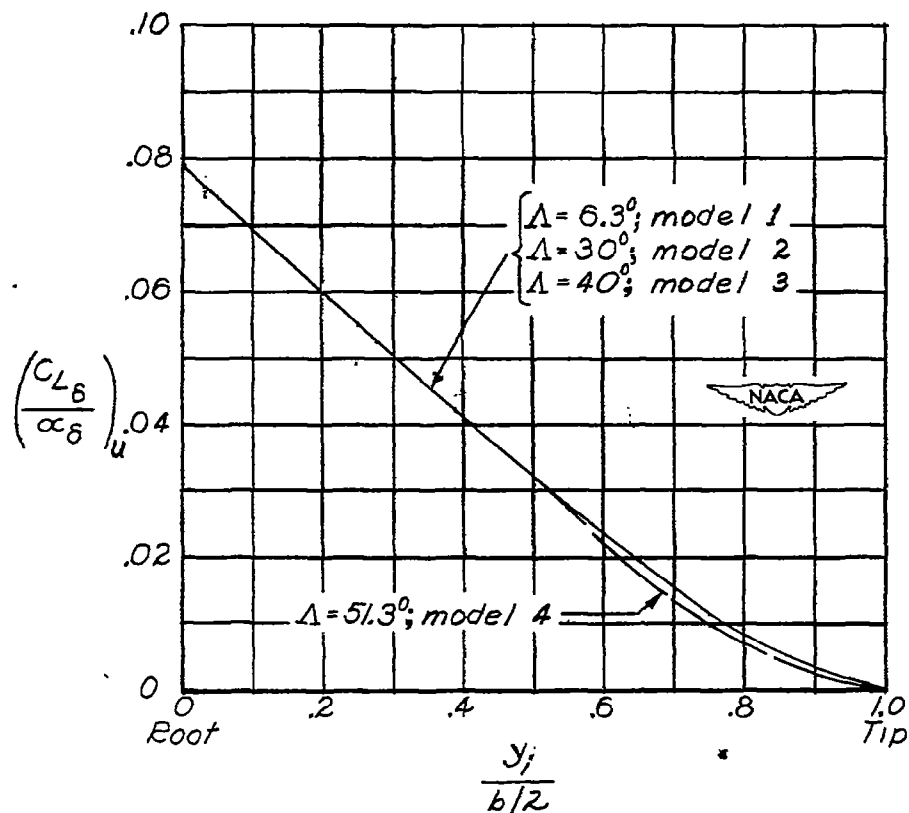
Figure 8.- Variation of experimental values of

$C_{L_\delta}/\alpha_\delta$ with flap span. $\dfrac{y_o}{b/2} = 1.00$;

$$C_{L_\delta} = \left(\dfrac{C_{L_\delta}}{\alpha_\delta}\right)_u \alpha_\delta K_3 \cos^2\Lambda .$$
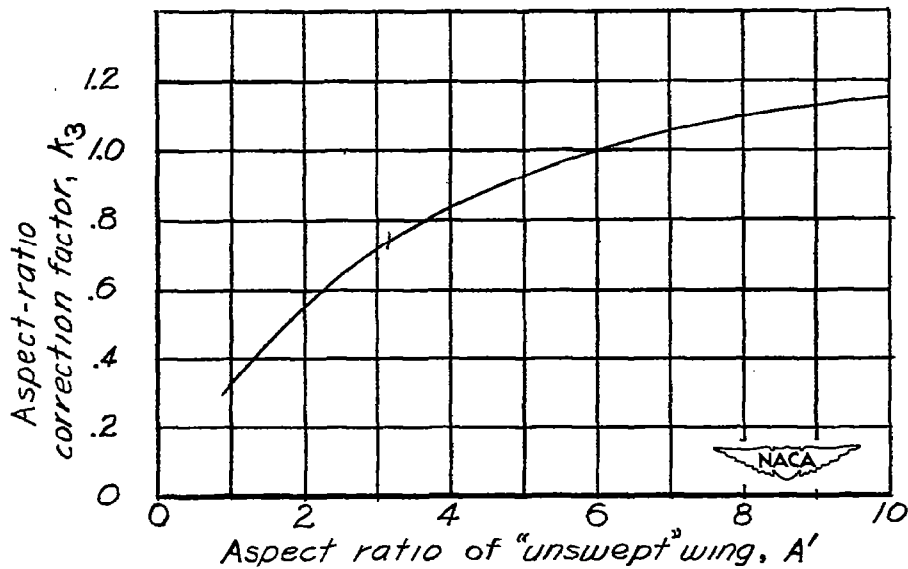
Figure 9.- Aspect-ratio correction factor for
calculating C_{L_δ}. (Curve based on data obtained

from the Langley 7- by 10-foot tunnel.)
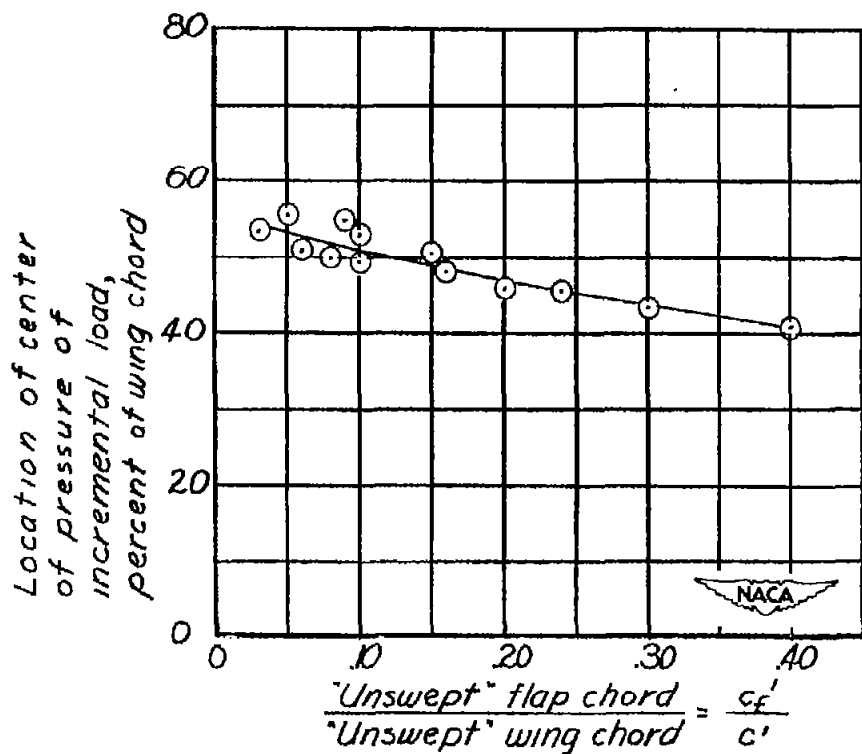
Figure 10.- Variation of center of pressure of incremental load with flap chord. (Data from references 8 to 11.)
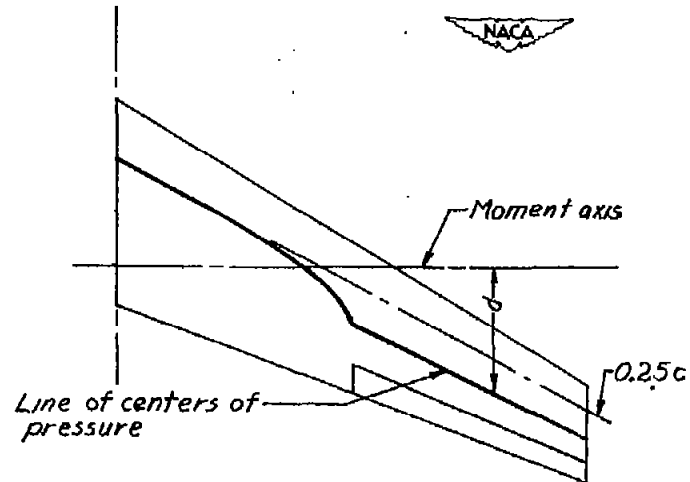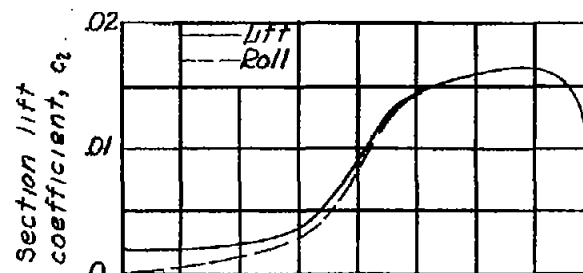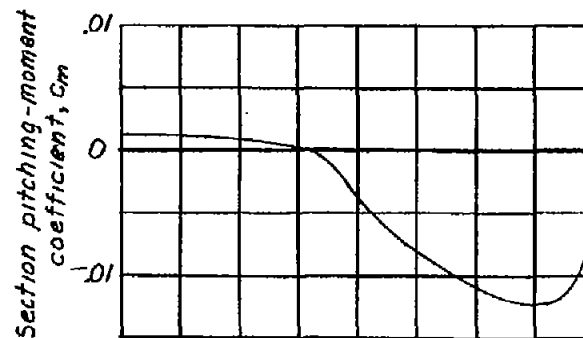
Figure 11.- Sample section lift and section pitching-moment coefficient distributions for a partial-span flap on a swept wing.
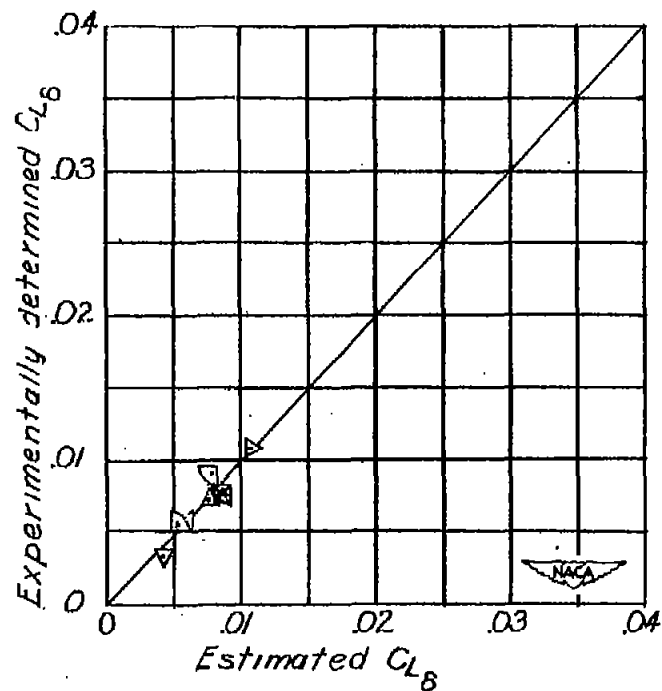
Figure 12.- Comparison of experimentally determined values of lift effectiveness parameter C_{L_δ} with values determined by method I. (Symbols refer to models listed in table I.)
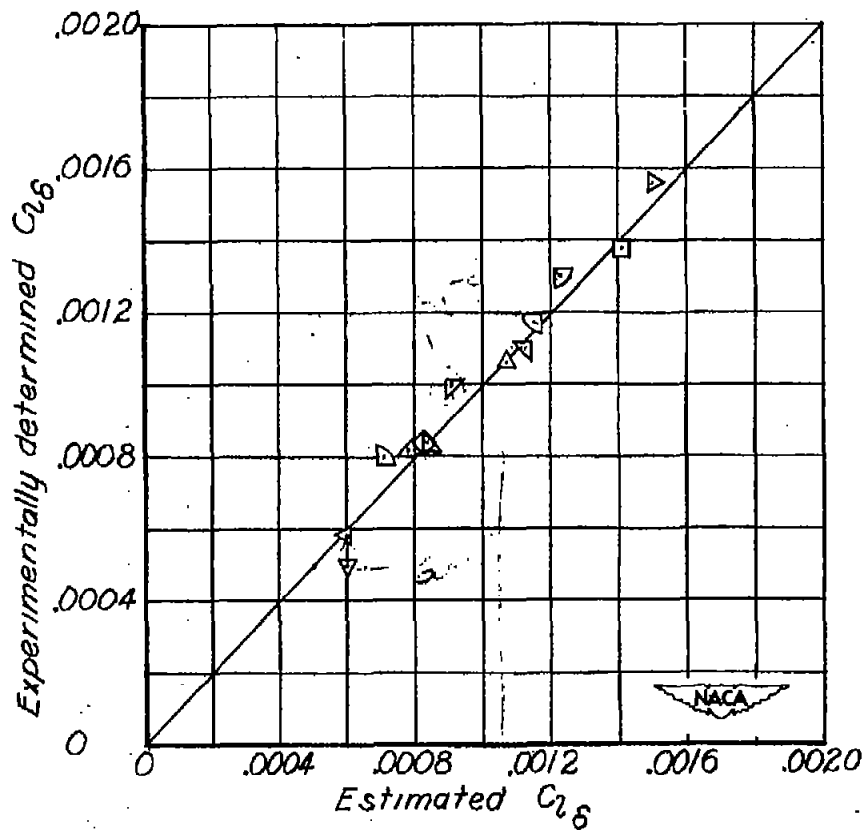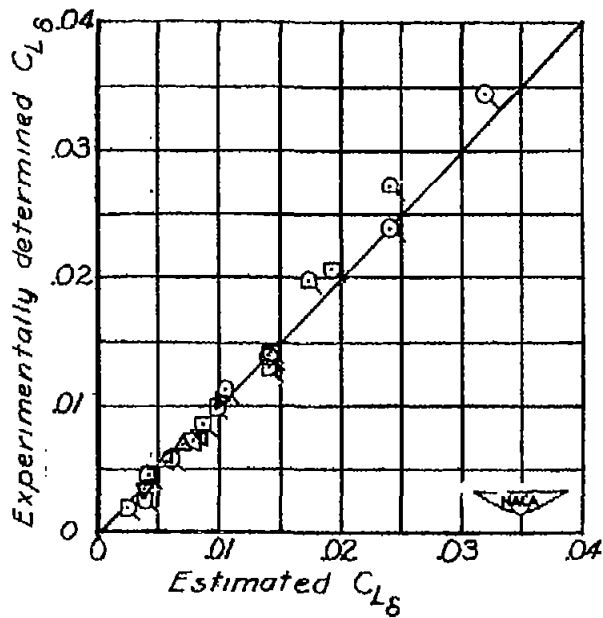
Figure 13.- Comparison of experimentally determined values of rolling effectiveness parameter C_{l_δ} with values determined by method I. (Symbols refer to models listed in table I.)

Figure 14.- Comparison of experimentally determined
values of lift effectiveness parameter C_{L_δ}

with values determined by method II. (Symbols
refer to models listed in table I. Flagged symbols
indicate comparison of estimated values with
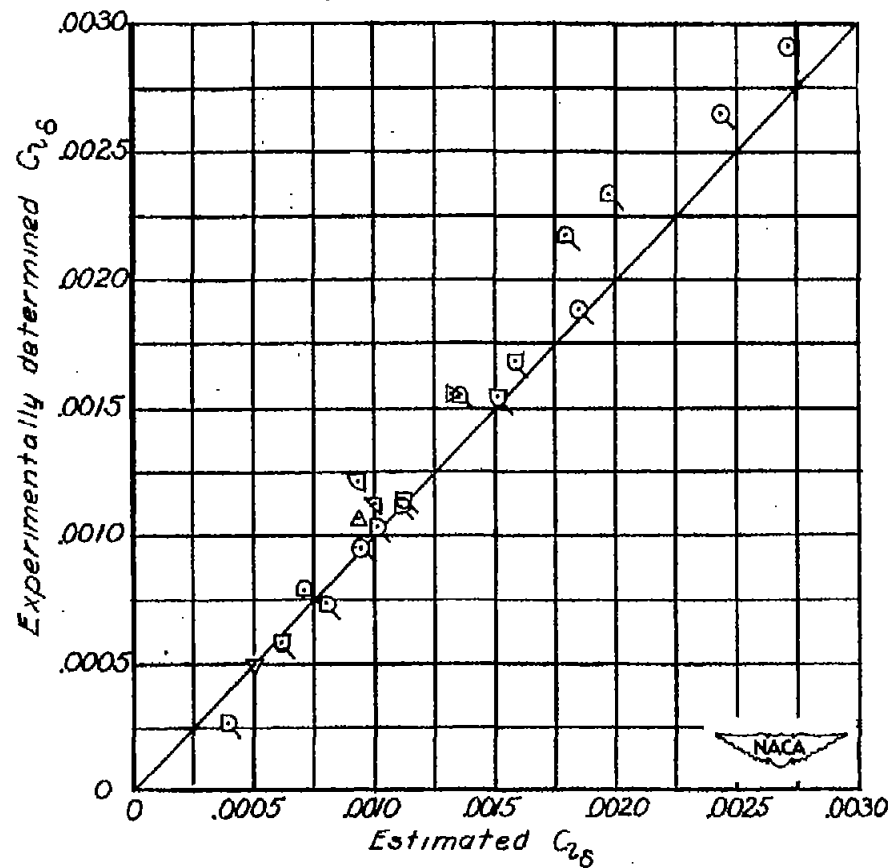faired curves of fig. 3.)

Figure 15.- Comparison of experimentally determined
values of rolling effectiveness parameter C_{l_δ}

with values determined by method II. (Symbols
refer to models listed in table I. Flagged symbols
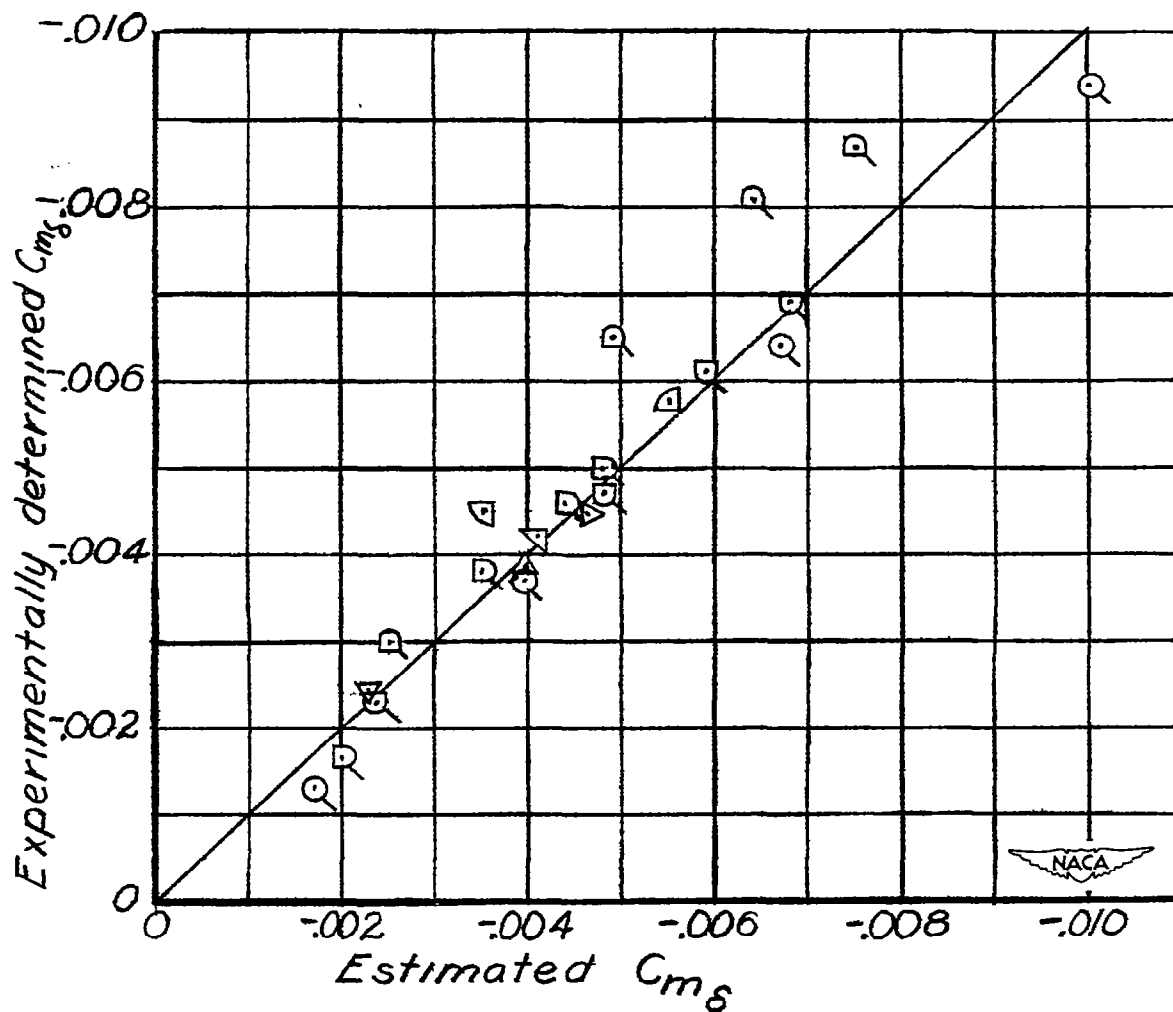indicate comparison of estimated values with
faired curves of fig. 2.)

Figure 16.- Comparison of experimentally determined values of
pitching effectiveness parameter C_{m_δ} with values determined

by method II. (Symbols refer to models listed in table I.
Flagged symbols indicate comparison of estimated values
with faired curves of fig. 4.)